ARTICLE

Supporting Information

PEDOT Coated Microneedle Towards Electrochemically assisted Skin Sampling

Siti Musliha Ajmal Mokhtar [a,b], Miko Yamada [a,c], Tarl W Prow [a,c], Mark Moore [d], Xanthe L Strudwick [a], and Drew R Evans*[a]

Morphology of MN after biased

PT/PS pair and SS/SS pair were tested with CA by applying +0.8 V to PEDOT:TOS as WE for 2 mins. For physical analysis, the morphology of MN was analysed using Scanning Electron Microscope (SEM). **Figure S1** showed morphology of PEDOT and stainless MN after CA for 2 mins with comparison to normal MN samples (without bias).

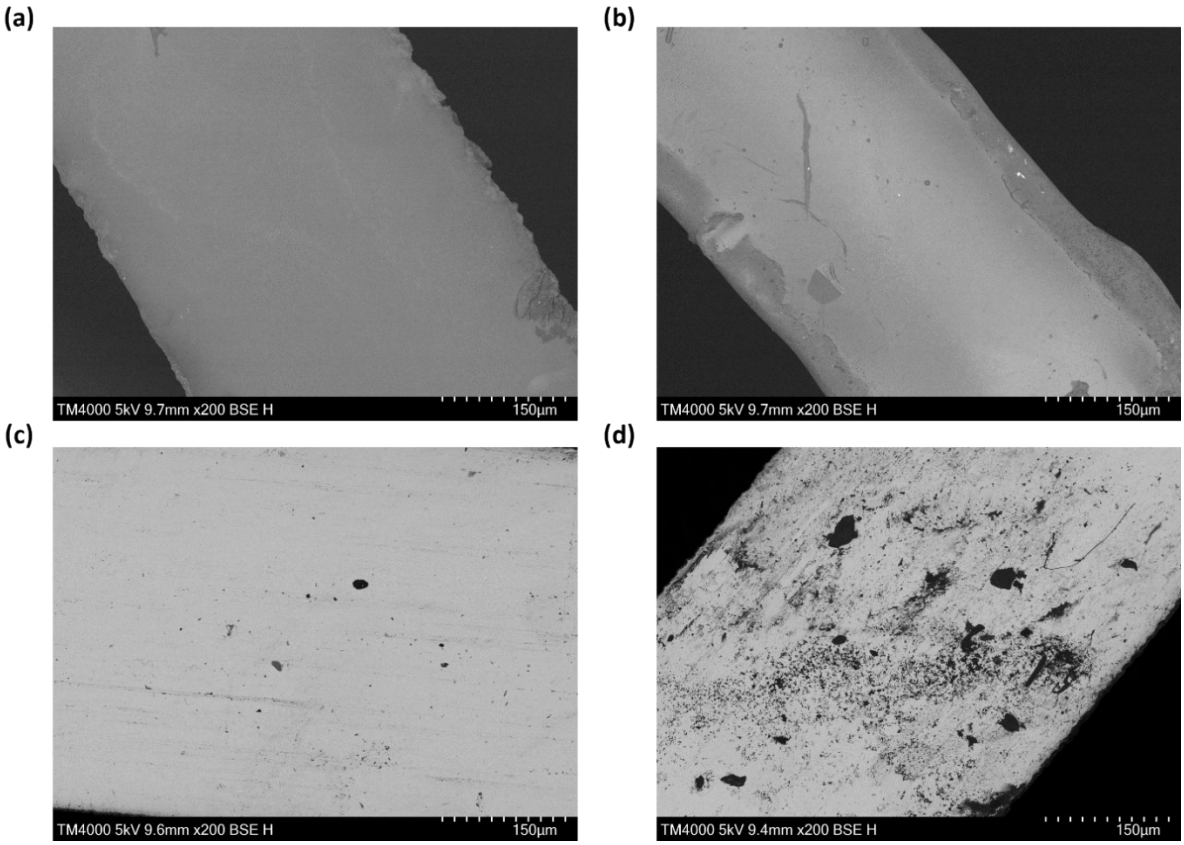

Figure S1. SEM image of MN tips. Surface conditions by SEM on PEDOT MN (a) untreated and (b) after bias, followed by stainless steel MN (c) normal and (d) after biased.

While there was minimal crack of PEDOT possibly due to coating defect, however, the polymer surface was much smoother than stainless steel. The mechanical degradation of stainless steel possibly resulted from corrosion due to CA procedure. As mentioned earlier, there was safety concern in using predecessor stainless steel MN in electrochemical assisted sampler. This result suggested possible metal ions released from the stainless-steel MN when potential was applied which hazardous in human body. Hence, following experiments would mainly discuss on PEDOT MN electrodes in the skin sampler.

MN penetration in Agarose gel

Detailed quantification of impedance versus penetration depth was analysed. Though PEDOT was studied as alternative to stainless steel, it is good to include the performance of stainless steel as control. This is significant to validate electrochemical performance of PEDOT as compared to conventional electroactive material, i.e. the stainless steel. Also, the mV potential in EIS has minimal risk to induce the corrosion of stainless steel. Different electrodes pairs for WE/CE were prepared using PEDOT:TOS/PEDOT:TOS (PT/PT) MNs, PEDOT:PSS/PEDOT:PSS (PS/PS) MNs and stainless steel/stainless steel (SS/SS) MNs. First, the electrodes were attached on dip coater rod, as controller to move MN electrodes into agarose gel. At each 100 µm insertion into the gel, the dip coater was stopped and EIS was run to measure the electrode's impedance. For simpler analysis, only high frequency range was conducted, from 100 Hz to 10 kHz based on previous study that conducted EIS for tissue layer discrimination.[1] **Figure S2a** showed impedance measured during 100 µm penetration increment into agarose gel at 10 kHz frequency. In general, the impedance reduced drastically towards 0.5mm penetration depth for every electrode, resulted from substantial increased of area at the triangle shape of the MN tip as seen in the inset. Then the impedance reduced steadily towards 2mm because the middle part of tip continuously moving into the gel. From 2mm onwards, the impedance was rather constant due to MN already reached the neck part and unable to go deeper into the gel. The overall impedance for PS/PS electrodes was higher than PT/PT and SS/SS where at 2mm depth, impedances for each electrode were 4.75 kΩ, 2.11 kΩ and 1.04 kΩ respectively. Though the impedances of PEDOT MNs were higher than stainless steel, the impedance trend was fairly the same.

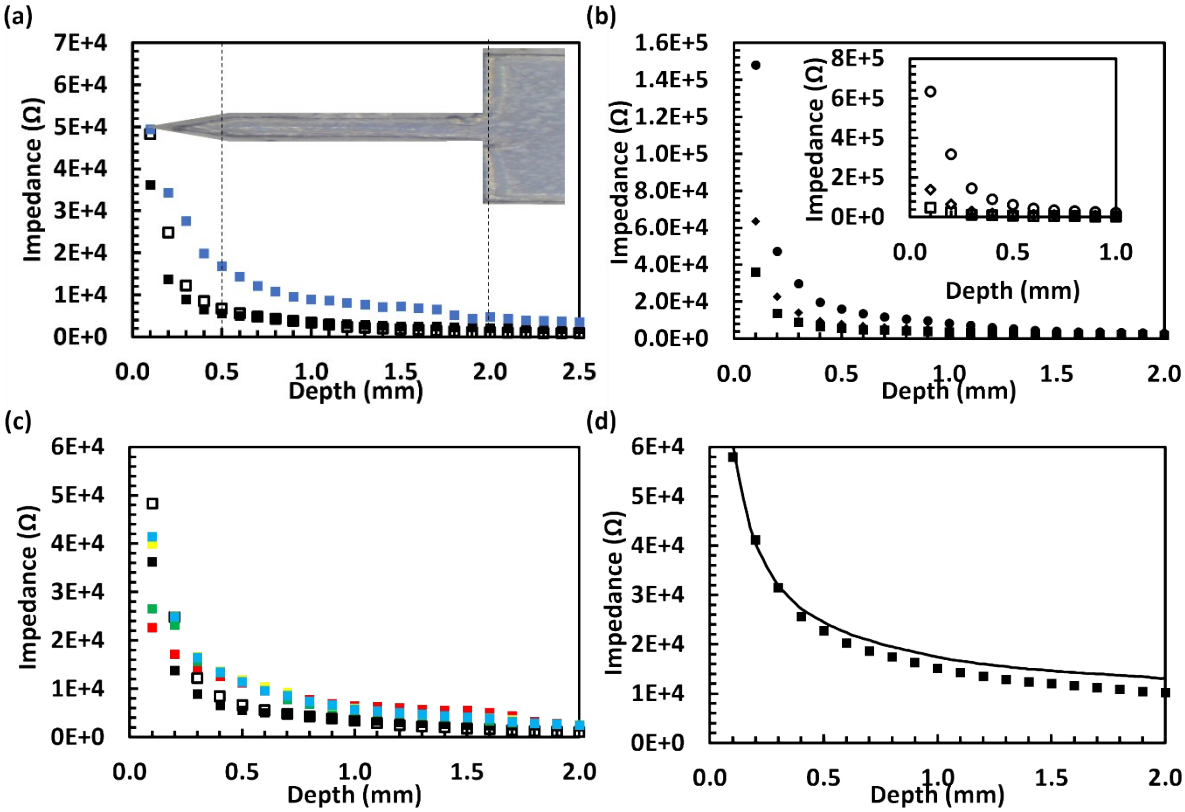

Figure S2. MN penetration depth sensing using EIS in agarose gel. (a) Impedance measured at 10 kHz over 100um incremented penetration depth controlled by dip coater into agarose gel for PEDOT:TOS (black), PEDOT:PSS (blue) and stainless steel (no filled). (b) Impedance of PEDOT:TOS over penetration depth measured at 10 kHz (square), 1 kHz (diamond) and 0.1 kHz (round). Inset showed impedance for stainless steel electrodes. (c) Impedance measured at 10 kHz of PEDOT:TOS made with different thickness by varying dip-coat's withdrawal speed (mm/min); 50 (black), 100 (red), 200 (green), 300 (yellow) and 500 (blue). Result is also compared with stainless steel (unfilled). (d) Impedance measured at 1 kHz of PEDOT:TOS during 100 µm depth increment sampling (no line) and instantaneous continuous reading (solid).

Another advantage of EIS was the electrical components that made up impedance value such as resistance and capacitance can be extracted through electrical equivalent circuit. For additional information on electrode's resistance and capacitance, broader range of input frequency from 0.1 Hz till 10 kHz was conducted as seen in Supplementary Data **Figure S3**. Due to long analysis time, only PT/PT and SS/SS electrodes were tested on just three penetration positions; when MNs started to pierce the gel, halfway in gel and fully in gel. **Figure S4** showed impedance remodelled using electrical equivalent circuit in which the resistance value decreased whereas capacitance value increased towards deeper penetration for both pairs.

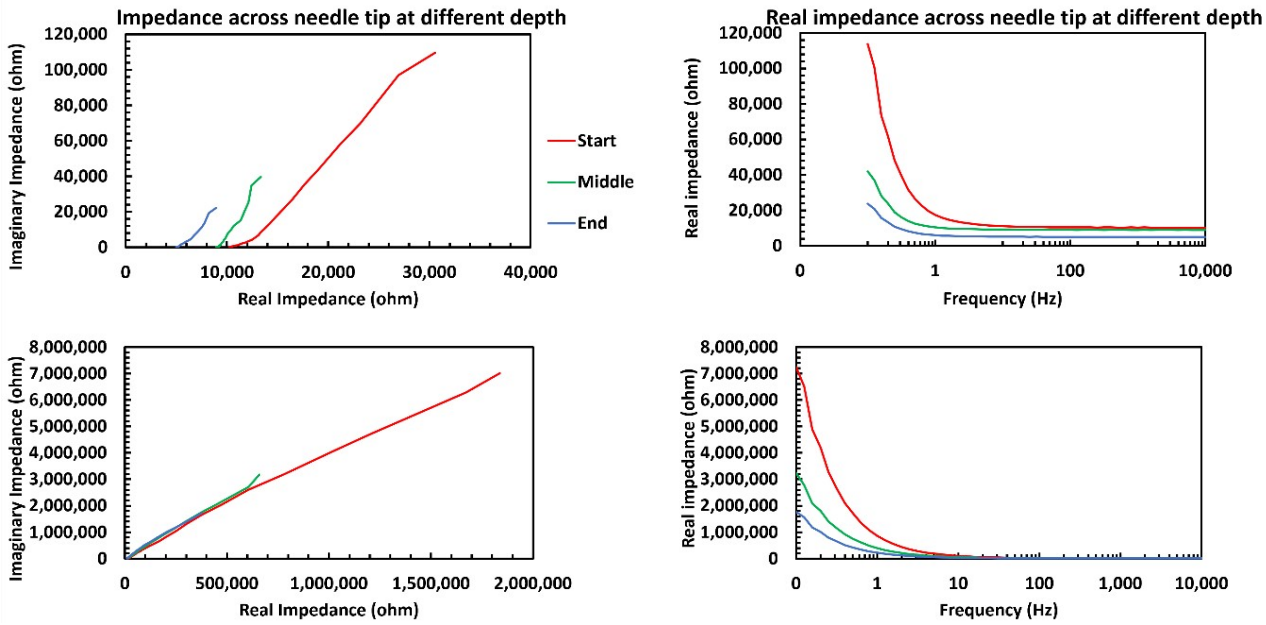

Figure S3. EIS impedance plot. Impedance plot consists of imaginary impedance versus real impedance, followed by real impedance versus frequency from 0.1 Hz to 10 kHz for PEDOT:TOS MNs in top and stainless-steel MN in bottom. Impedance are read at three MN penetration levels; start to pierce (red), halfway pierced (green) and fully pierced (blue).

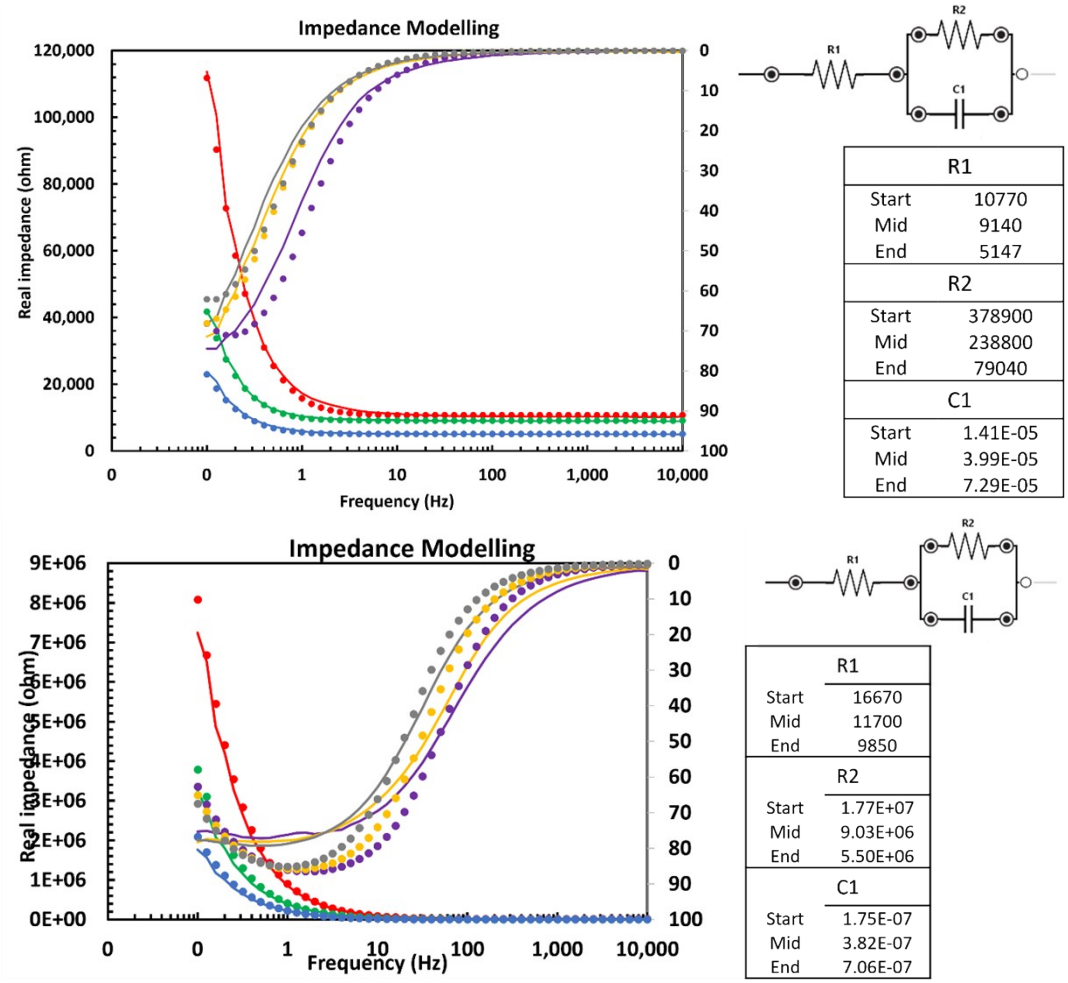

	R1
Start	10770
Mid	9140
End	5147
	R2
Start	378900
Mid	238800
End	79040
	C1
Start	1.41E-05
Mid	3.99E-05
End	7.29E-05

	R1
Start	16670
Mid	11700
End	9850
	R2
Start	1.77E+07
Mid	9.03E+06
End	5.50E+06
	C1
Start	1.75E-07
Mid	3.82E-07
End	7.06E-07

Figure S4. EIS impedance plot. Impedance plot consists of imaginary impedance (right axis) and real impedance (left axis) with experimental data (dotted) and modelling data (solid). Electrical equivalent circuit including its component values are shown in table during three MN penetration levels; start to pierce (red), halfway pierced (green) and fully pierced (blue). Top figures for PEDOT:TOS MNs and bottom figures for stainless steel MN.

Another thing to note was impedance value can vary depending on the frequency of the input signal even in bio tissue,[2] hence **Figure S2b** showed trend of impedance against input signal frequency for both PT/PT and SS/SS electrodes (inset). In both electrodes, input frequency of 10 kHz showed lowest impedance compared to 1 kHz and 0.1 kHz especially in early penetration. Similar observation reported in EIS based bio tissue depth profiling study. [1, 3] Next, in real microfabrication practise, there was possibility of coating parameters variations in the microsize substrate such as thickness. It was reported that different thickness of PEDOT coating resulted in difference of EIS impedance.[4] To investigate PEDOT electrodes performance across thickness variations, few PEDOT:TOS MNs with different coating thicknesses were prepared using different dip-coat's withdrew speed (mm/min); 50, 100, 200, 300 and 500 in which slower withdrew speed resulted in thicker PEDOT coating. **Figure S2c** showed impedance at 100um penetration depth increment in agarose gel for all PEDOT:TOS electrodes including stainless steel electrode as reference. Though the thickness varies, minimal impedance change was observed. In other word, it was reassured to note that variability of coating thickness in actual fabrication does not majorly affect the impedance change.

In previous experiments, the movement of MN was paused at each 100um increment to allow reading of impedance. In real practise, it was essential to make sure impedance was readable over time period when MN was punctured into skin. To prove impedance readability and reliability of PEDOT MN sampler in actual scenario, the electrodes was inserted continuously into agarose gel at insertion speed of 8um/sec and impedance was read during the whole insertion period without any pause. **Figure S2d** showed good comparison of impedance between 100 um sampling from previous experiment and during instantaneous reading. The slight difference possibly resulted from gel drying over time.

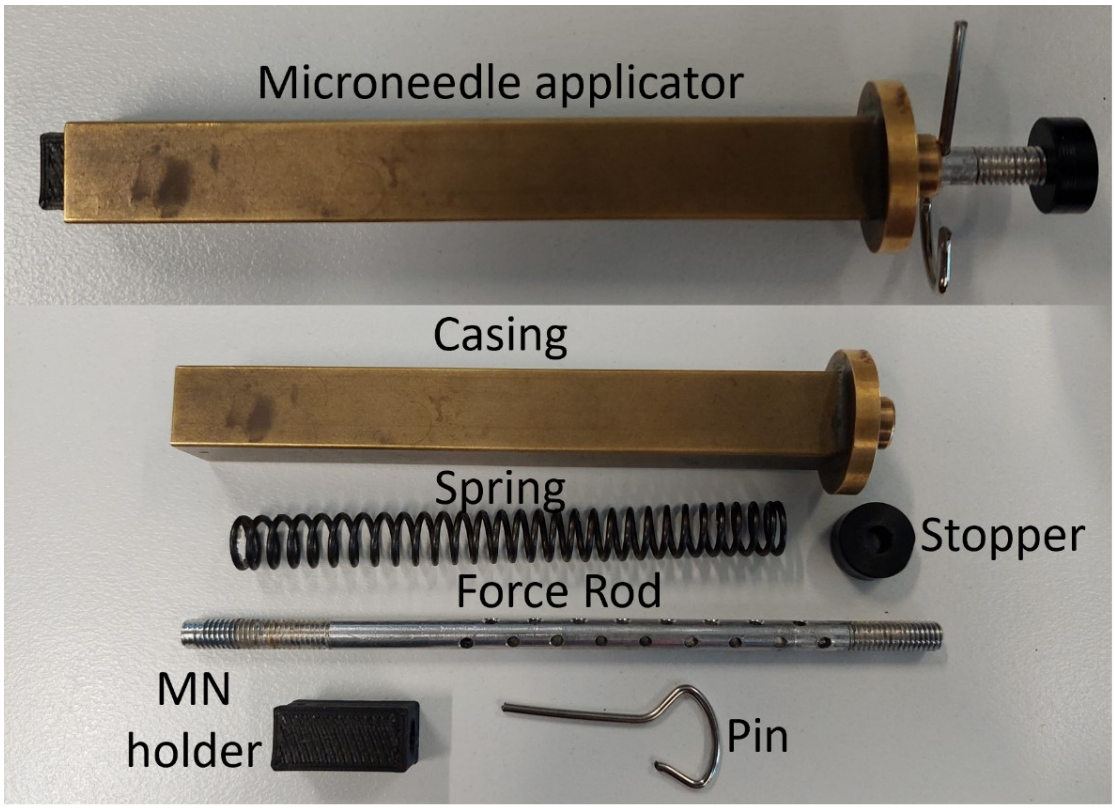

Figure S5. Microneedle applicator design. Applicator consisted of spring-loaded force rod with MN holder and stopper attached at each end of the rod, enclosed inside the casing. MN release force was controlled by pulling the rod out from the casing, thus compressing the spring. Pin then inserted into the hole on force rod to hold the compressed spring. When pin was taken out from rod, spring then expanded thus pushing MN holder into skin.

Selection of PEDOT's MN potential

As discussed above, CV and CA would be employed to the MN sampler for ISF extraction. In CV, a cycle potential range was applied to electrodes and response current was measured to observe redox potential of PEDOT. The redox potential then used in CA for actual ISF extraction based on reverse iontophoresis concept. Before start, it was worth to note that the MN would be in contact within skin layer, made up by stratum corneum, epidermis and dermis.[5] For extraction of ISF, it was important to make sure MN was punctured into skin and reached the dermis layer to access ISF. Therefore, EIS was conducted prior to every experiment to determine MN depth in the skin. **Figure S6a** showed typical voltammogram graph measured when CV was applied. The inset showed EIS impedance prior to experiment, with value around 5 kΩ, which comparable to previous experiment. The potential was increased from -1V to 1 V, referred to as oxidative scan which

then swept back to -1 V, referred as reductive scan with scan rate of 100 mv/s. In the current response, two peaks had been observed at 0.8 V during oxidative scan and -0.8 V during reductive scan, possibly indicated oxidation and reduction potential of PEDOT in the skin.

Regarding two electrodes system employed in the skin sampler, though it offered simplest setup, there was disadvantage of limited control of the WE potential. In this system, CE was used to complete the circuit by allowing charge to flow through the system and to maintain constant potential between electrolyte and the WE. However, at higher current, potential of CE changed hence limiting potential applied at the WE.[6] This would not be issue in EIS as only small signal was used. In contrast, CA and CV employed larger potential hence the actual WE potential might be smaller than 0.8V or -0.8V. Comparison between two and three electrodes system of PEDOT performance was observed in supplementary **figure S7**, showing shifting of peak potential and different peak currents between the systems resulted from the difference of actual WE potential in both systems.

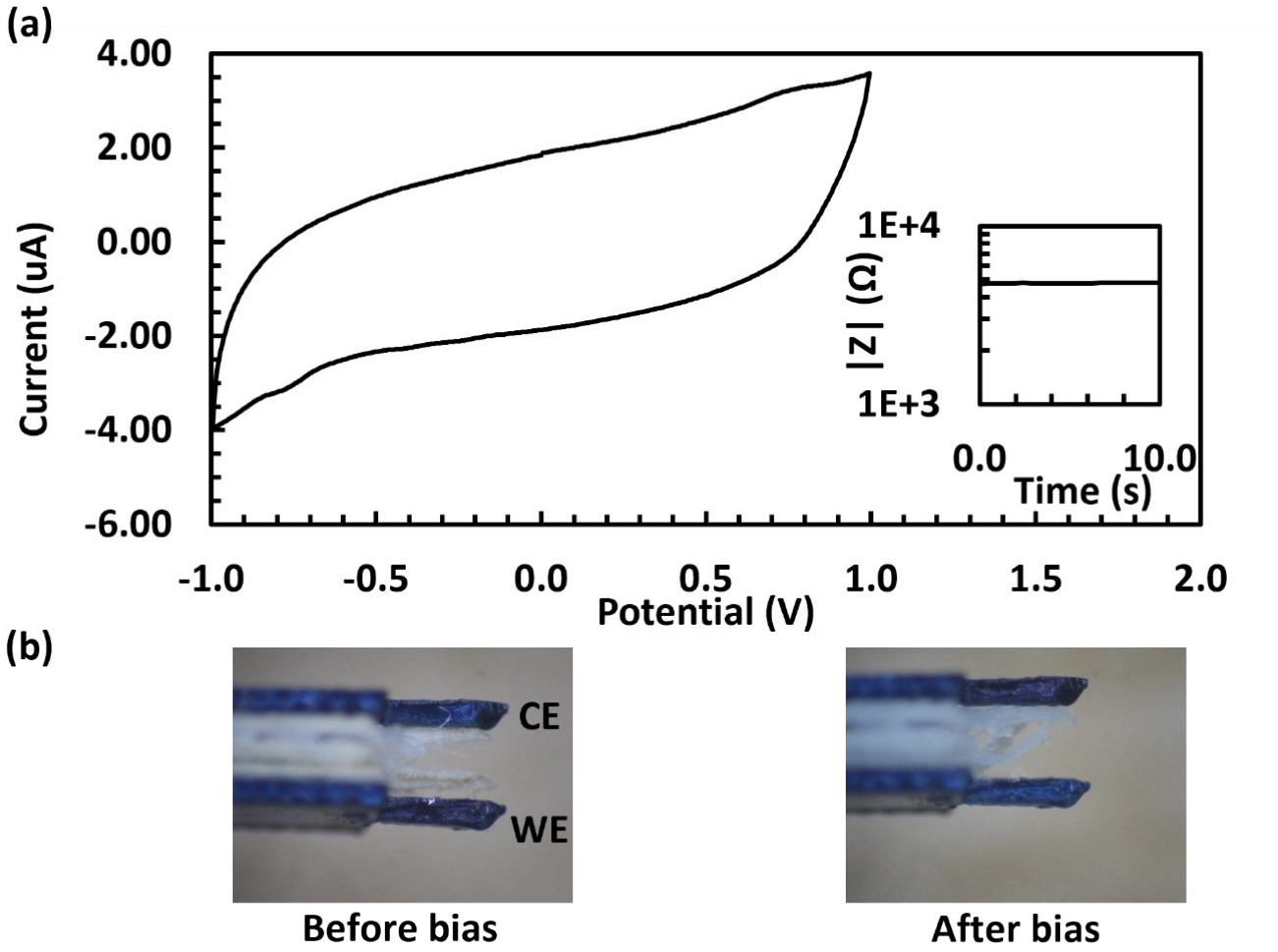

Figure S6. Selecting potential to apply on PEDOT in the skin. (a) CV of PEDOT:TOS MN in skin. Inset showed impedance measured at 5 kΩ confirming PEDOT was in skin prior to CV measurement. (b) PEDOT:TOS MN with colour changed before and after CA at 0.8 V (PEDOT peak potential from a) for 1 min.

To further investigate on the PEDOT redox potential, CA was conducted on PT/PT electrodes at 0.8 V for 1 min due to the fact that PEDOT has electrochromic property where its colour changes when reduced/oxidized.[7] **Figure S6b** showed PEDOT:TOS colour change before and after CA. PEDOT:TOS at WE turned lighter, which indicated oxidation of the PEDOT while PEDOT:TOS at CE turned darker, indicating reduction on the PEDOT. This observation suggested that though the actual potential probably smaller than 0.8 V, it still over the redox potential of PEDOT at both CE and WE. This is important to make sure PEDOT would change according to previously explained experimental setup.

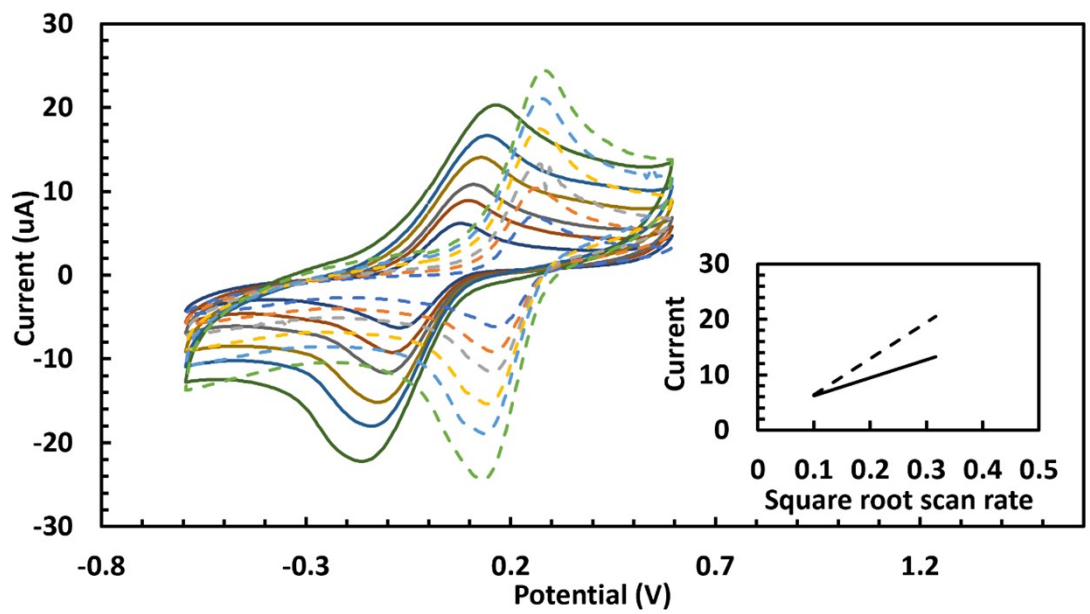

Figure S7. Comparison between 2 electrode and 3 electrode system. Cyclic voltammetry of WE: PEDOT:TOS MN, CE: Pt wire and RE: Ag/AgCl, at different scan rates (mV/s); 10 (dark blue), 20 (red), 30 (grey), 50 (dark yellow), 70 (blue) and 100 (dark green) for 2 electrodes (solid) and 3 electrodes (dashed). Inset showed peak current between 2 electrode (solid) and 3 electrodes (dashed). Electrolyte is 0.5 mM ferri/ferrocyanide in artificial ISF.

ISF extraction in Skin Sampler

In this section, the volume of extracted ISF was analyzed to investigate if reverse iontophoresis in the skin sampler possible to enhance the extraction. First, 3 sets of PEDOT sampler without CA as control were tested, namely 1st ~ 3rd followed by another 3 sets with CA at 0.8V for 2 mins, namely 4th ~ 6th. As indicated previously, it was important to make sure MN was fully inserted into skin by observing the impedance value. Hence, prior to each extraction, EIS was conducted for 10sec to read the impedance. The impedance value and image of absorbent paper were shown in **Figure S8**. In **Figure S8a**, though experiment setups were same, there were quite significant variance of the impedance prior each extractions, possibly due to complex topography and texture of the skin, e.g. skin thickness and elasticity hindering MN penetration.[8] Hence for fair comparison between bias and control, only extractions with most similar impedance (~3 kΩ - 5 kΩ) are selected which are 3rd, representing control and 4th, representing bias sampler.

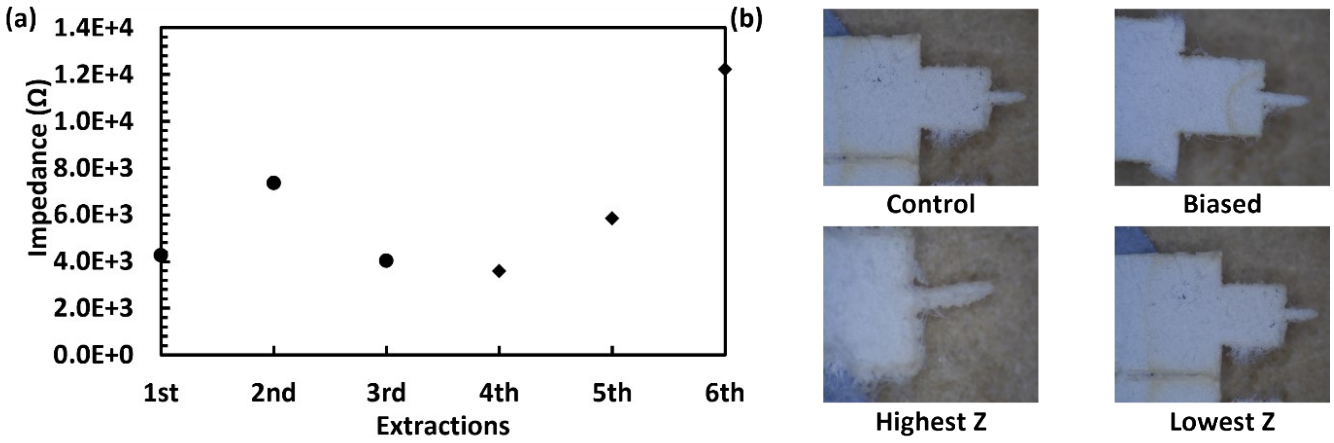

Figure S8. ISF extraction using PEDOT MN. Impedance measured prior to control (round) and biased (diamond) extraction using PEDOT:TOS/PEDOT:PSS MNs. (b) Microscope image of absorbent layer with stained indicating extracted ISF for control and biased extraction, also for extractions with highest and lowest impedance in control sampler.

Figure S8b showed microscopy image of the absorbent paper after extraction process where the stained area was used to approximate amount of ISF extracted. Unfortunately, in oppose to previous theory, control sampler collected more ISF as compared to biased sampler. This might be due to the effect of capillary pressure by the absorbent paper towards ISF was much higher than the effect of the electroosmosis pressure. This was in agreement with previous work reporting Whatman filter paper had great water absorptiveness due to its wicking ability.[9] To further investigate on capillary pressure only, control sampler with lowest and highest impedance were compared in **Figure S9**. As discussed earlier, lower impedance indicated deeper penetration and otherwise. When MN inserted deeper in skin, larger area

of MN cum absorbent paper was exposed to ISF in the skin allowing higher capillary pressure of absorbent paper towards ISF and hence more ISF was collected. It was observed that control sampler with lowest impedance has larger stained area and otherwise.

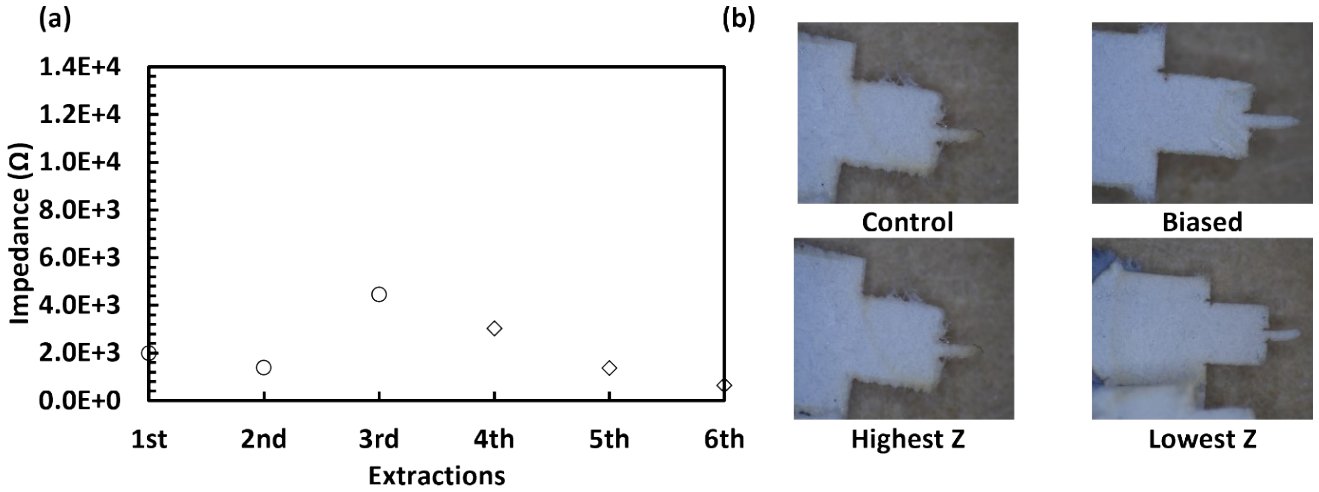

Figure S9. ISF extraction using stainless steel sampler. Impedance measured prior to control (round) and biased (diamond) extraction using stainless steel MNs. (b) Microscope image of absorbent layer with stained indicating extracted ISF for control and biased extraction, also for extractions with highest and lowest impedance in control sampler.

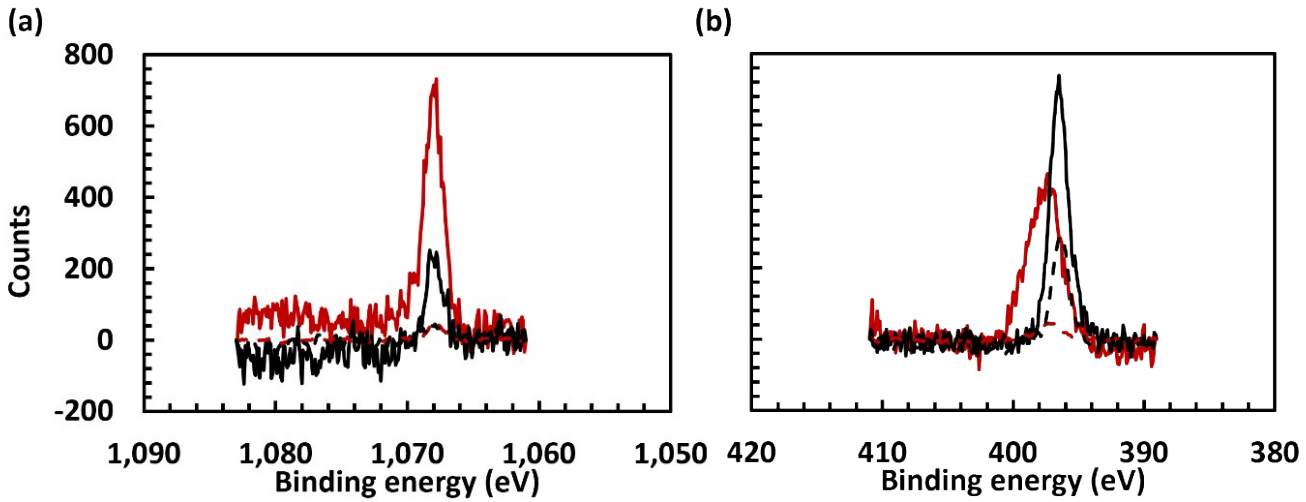

Figure S10. Surface analysis of XPS on MN sampler. Fine scan analysis of (a) Na1s and (b) N1s on anode (red) and cathode (black) biased PEDOT sampler (solid) and stainless-steel sampler (dashed).

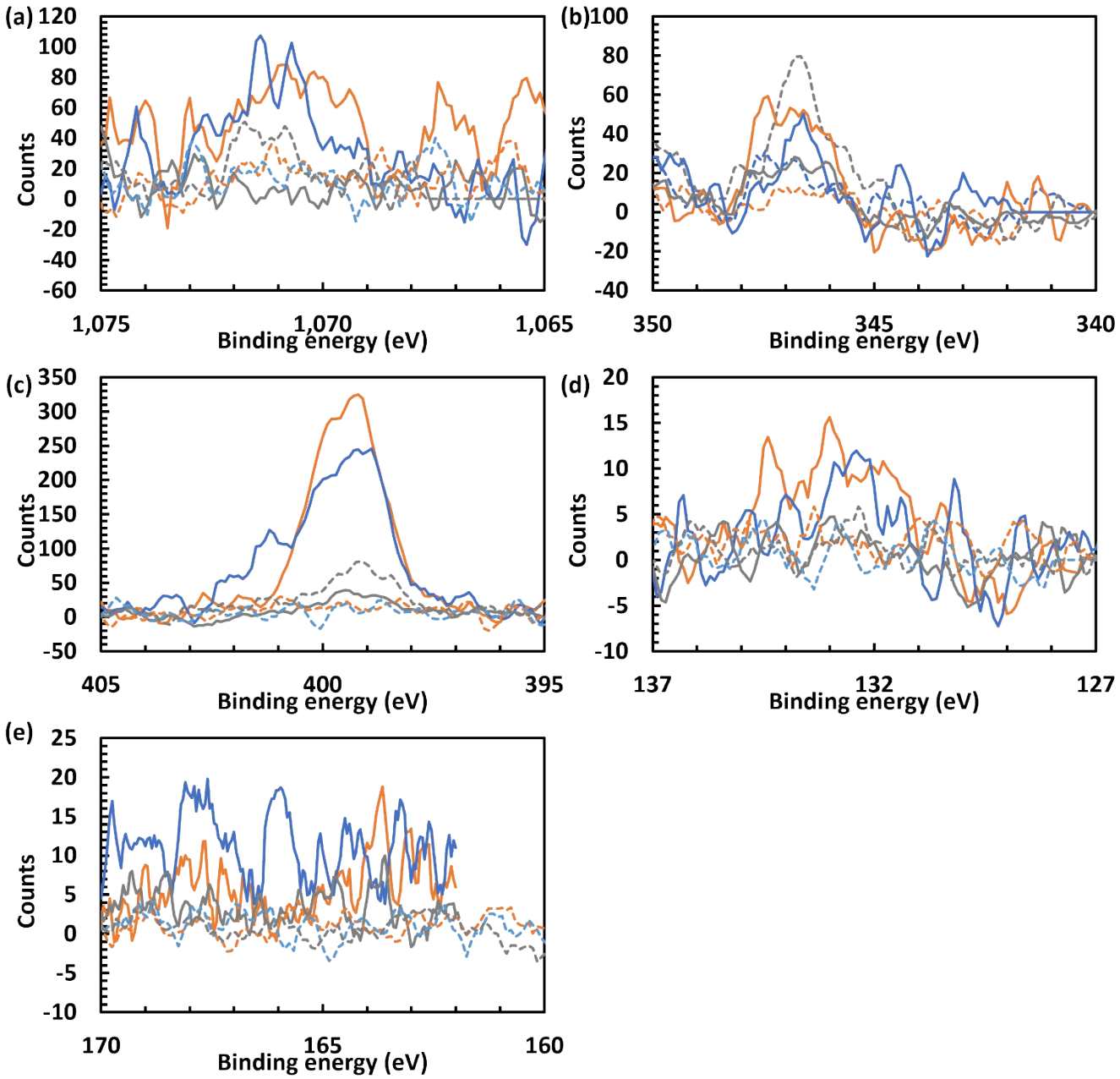

Figure S11. Surface analysis of XPS on absorbent paper. Fine scan analysis of (a) Na1s, (b) Ca2p, (c) N1s, (d) P2p and (e) S2p of biased (solid) and no bias (dashed) PEDOT MN sampler. Paper adjacent to PEDOT:TOS (orange), middle paper (blue) and paper adjacent to PEDOT:PSS (grey).

References

1. J. Yun, G. Kang, Y. Park, H. W. Kim, J.-J. Cha and J.-H. Lee, *Sensors and Actuators B: Chemical*, 2016, **237**, 984-991.
2. J. Kim, J. Yun, H.-H. Cho and J.-H. Lee, *Journal of Electroanalytical Chemistry*, 2019, **838**, 48-56.
3. J. Yun, H. W. Kim and J. H. Lee, *Sensors (Basel)*, 2016, **16**.
4. G. Dijk, H. J. Ruigrok and R. P. O'Connor, *Advanced Materials Interfaces*, 2020, **7**.
5. T. Waghule, G. Singhvi, S. K. Dubey, M. M. Pandey, G. Gupta, M. Singh and K. Dua, *Biomed Pharmacother*, 2019, **109**, 1249-1258.
6. M. Pohanka and P. Skládal, *Journal of Applied Biomedicine*, 2008, **6**, 57-64.
7. D. Levasseur, I. Mjejri, T. Rolland and A. Rougier, *Polymers (Basel)*, 2019, **11**.

8. P. Makvandi, M. Kirkby, A. R. J. Hutton, M. Shabani, C. K. Y. Yiu, Z. Baghbantaraghdari, R. Jamaledin, M. Carlotti, B. Mazzolai, V. Mattoli and R. F. Donnelly, *Nanomicro Lett*, 2021, **13**, 93.
9. C. Kolluru, M. Williams, J. Chae and M. R. Prausnitz, *Adv Healthc Mater*, 2019, **8**, e1801262.

